Article

Fusion-Assisted Hydrothermal Synthesis and Post-Synthesis Modification of Mesoporous Hydroxy Sodalite Zeolite Prepared from Waste Coal Fly Ash for Biodiesel Production

Juvet Malonda Shabani [1], Alechine E. Ameh [1], Oluwaseun Oyekola [1,*], Omotola O. Babajide [2] and Leslie Petrik [1,3]

[1] Department of Chemical Engineering, Cape Peninsula University of Technology, Cape Town 7535, South Africa
[2] Department of Mechanical Engineering, Cape Peninsula University of Technology, Cape Town 7535, South Africa
[3] Environmental and Nano Science Research Group, University of Western Cape, Cape Town 7535, South Africa
[*] Correspondence: oyekolas@cput.ac.za; Tel.: +27-(0)-21-959-6799

Abstract: Increases in biodiesel prices remains a challenge, mainly due to the high cost of conventional oil feedstocks used during biodiesel production and the challenges associated with using homogeneous catalysts in the process. This study investigated the conversion of waste-derived black soldier fly (BSF) maggot oil feedstock over hydroxy sodalite (HS) zeolite synthesized from waste coal fly ash (CFA) in biodiesel production. The zeolite product prepared after fusion of CFA followed by hydrothermal synthesis (F-HS) resulted in a highly crystalline, mesoporous F-HS zeolite with a considerable surface area of 45 m^2/g. The impact of post-synthesis modification of the parent HS catalyst (F-HS) by ion exchange with an alkali source (KOH) on its performance in biodiesel production was investigated. The parent F-HS zeolite catalyst resulted in a high biodiesel yield of 84.10%, with a good quality of 65% fatty acid methyl ester (FAME) content and fuel characteristics compliant with standard biodiesel specifications. After ion exchange, the modified HS zeolite catalyst (K/F-HS) decreased in crystallinity, mesoporosity and total surface area. The K/F-HS catalyst resulted in sub-standard biodiesel of 51.50% FAME content. Hence, contrary to various studies, the ion exchange modified zeolite was unfavorable as a catalyst for biodiesel production. Interestingly, the F-HS zeolite derived from waste CFA showed a favorable performance as a heterogeneous catalyst compared to the conventional sodium hydroxide (NaOH) homogeneous catalyst. The zeolite catalyst resulted in a more profitable process using BSF maggot oil and was economically comparable with NaOH for every kilogram of biodiesel produced. Furthermore, this study showed the potential to address the overall biodiesel production cost challenge via the development of waste-derived catalysts and BSF maggot oil as low-cost feedstock alternatives.

Keywords: coal fly ash; zeolite; hydroxy sodalite; fusion-assisted hydrothermal; ion exchange modification; catalyst; BSF oil; heterogeneous catalyst; sodium hydroxide; biodiesel

1. Introduction

Biodiesel is a promising alternative renewable energy source with potential to supplement or substitute finite and highly polluting fossil fuels [1]. The utilization of biodiesel demonstrates a greener and more sustainable form of energy [2,3]. Its cost remains a major challenge vis-à-vis its counterpart, petroleum diesel [2]. Costs of oil feedstock, and purification of biodiesel products derived from the conventional homogeneous catalyst, are major contributors to the total production cost of biodiesel [3–5]. The drawbacks associated with conventional biodiesel production emphasize the need to explore a sustainable approach for cost competitive biodiesel production. Waste-derived black soldier fly (BSF) maggot oil has the potential to be transformed into biodiesel [6,7], and is employed as

feedstock in the current study. The maggot oil was derived from BSF insects that feed on organic wastes [8,9]. Compared to other biodiesel waste oil feedstocks [2,3,10], the use of the BSF oil comes with the advantage of being generated and possibly supplied at large industrial scale-volume. BSF oil is generated as a by-product during the production of protein meal from BSF, with a current output estimated at over 50 tonnes per annum in South Africa [11,12].

Coal fly ash (CFA) is a low cost and abundant solid waste generated as a by-product from coal combustion [13,14]. CFA has been used as a feedstock for the production of zeolites [15–17]. In South Africa alone, it is estimated that over 35 Mt of coal fly ash is generated annually, of which only one-tenth is recycled for use [18,19]. This waste can be utilized to synthesize zeolites, benefitting the environment and the economy. Using CFA as a low-cost feedstock source for catalyst development could also aid in minimizing the production cost of biodiesel. The application of zeolites in biodiesel production has gained attention [20–22], such that these catalysts are "probably the most investigated inorganic solid acid catalysts for the production of biodiesel by transesterification" [23]. The commonly reported zeolites used as catalysts in biodiesel production include MFI, BEA, ZRP and FAU type zeolite [21,24,25]. These zeolites typically have 10-membered or 12 membered pore openings defining their micropore sizes that are generally accessible to smaller organic molecules, whereas HS has a four–membered ring pore opening, making its very small micro pore structure relatively inaccessible to organic molecules [26,27]. Due to the ability to control the acidic characteristics of zeolites, several studies have been conducted to enhance their activity in biodiesel production [23,28]. The main route to control their acid sites involves the exchange of the cations contained in their aluminosilicate cages with either a proton or an alkali metal source [20,23]. For example, Xie, et al. [29], Babajide, et al. [30] and Volli and Purkait [25] ion-exchanged Na-X zeolite with K^+ using potassium hydroxide (KOH) and potassium acetate (CH_3COOK) as an alkali metal source, respectively, to enhance the basic strength (basicity) of the catalysts to favour the biodiesel transesterification reaction and improve biodiesel yield. In a study by Sivasamy et al. [23] and by Sun et al. [21], various Na-zeolites (MOR, MFI, FAU, and BEA) were ion exchanged by protonation with H^+ (i.e., converted to H-type) using ammonium chloride (NH_4Cl) as a proton source. Both resulted in a higher biodiesel yield that solely depended on the obtained increased acid strength of the catalyst. However, the exclusion of the ion exchange modification step in the case of HS zeolite is being investigated for the first time in this study.

The textural properties of zeolites are characteristics that promote their use in catalytic applications [23,31]. Many studies have proven that conditions applied during zeolite synthesis influence the resultant characteristics [31–34]. Bukhari, Behin, Kazemian and Rohani [32] and Mezni et al. [35], in separate studies, synthesised zeolites via fusion followed by hydrothermal conditions (a fusion-assisted hydrothermal method). The zeolites were associated with higher BET surface area, higher cation exchange capacity (CEC), and higher mesoporosity compared to zeolite obtained via the direct method. These findings have motivated the use of the fusion-assisted hydrothermal method for the synthesis of HS zeolite to be used as a catalyst in biodiesel production in this study. To our knowledge, no published study examines the fusion-assisted hydrothermal process followed by post-synthesis ion-exchange modification of HS made from CFA for biodiesel production.

Hydroxy sodalite (HS) is a zeolite form with strong basic sites [26,31], with only two attempts reported for its use as a catalyst in biodiesel production [36,37]. In the study by Makgaba and Daramola [36], the HS zeolite was hydrothermally synthesized from pure chemical reagents using the conventional direct hydrothermal method; the study showed only preliminary results and catalytic potential of the zeolite in biodiesel production. HS zeolite consists of β-cages (sodalite cages) that enclose four-ring apertures, and the material possesses a small number of framework units (based on Si/Al ratio) [26,27]. HS zeolite thus has a small pore size (2.8 Å), resulting in a more condensed structure compared to its counterpart zeolites (MFI ZMS-5, 32 Å; FAU Na-X, 7.3 Å) [26,38] commonly explored in

biodiesel production. Based on the above, the material is assumed to have a sufficient external surface area with available catalytic sites suitable for biodiesel conversion [39]. It could also be cheaper (with reference to material requirements) and easier to synthesize (with reference to its framework and non-requirement of structure directing agents) compared to counterpart medium and large pore zeolites [24]. Thus, in this study the HS material is investigated for its potential to counteract high biodiesel production costs caused by use of conventional zeolites or homogenous catalysts.

2. Results and Discussion

HS was synthesized from CFA via a fusion-assisted hydrothermal method, followed by post-modification by ion exchange of the obtained product, as described in Section 3.2. The details of the experimental procedure are given in Sections 3.2.1 and 3.2.2 respectively. This section presents and discusses the XRD, SEM-EDS, FT-IR and textural characterization of the synthesized products.

2.1. XRD Analysis

Figure 1 presents the XRD patterns of CFA, the hydrothermal fusion assisted-derived zeolite (F-HS), and the modified ion-exchanged product (K/F-HS)
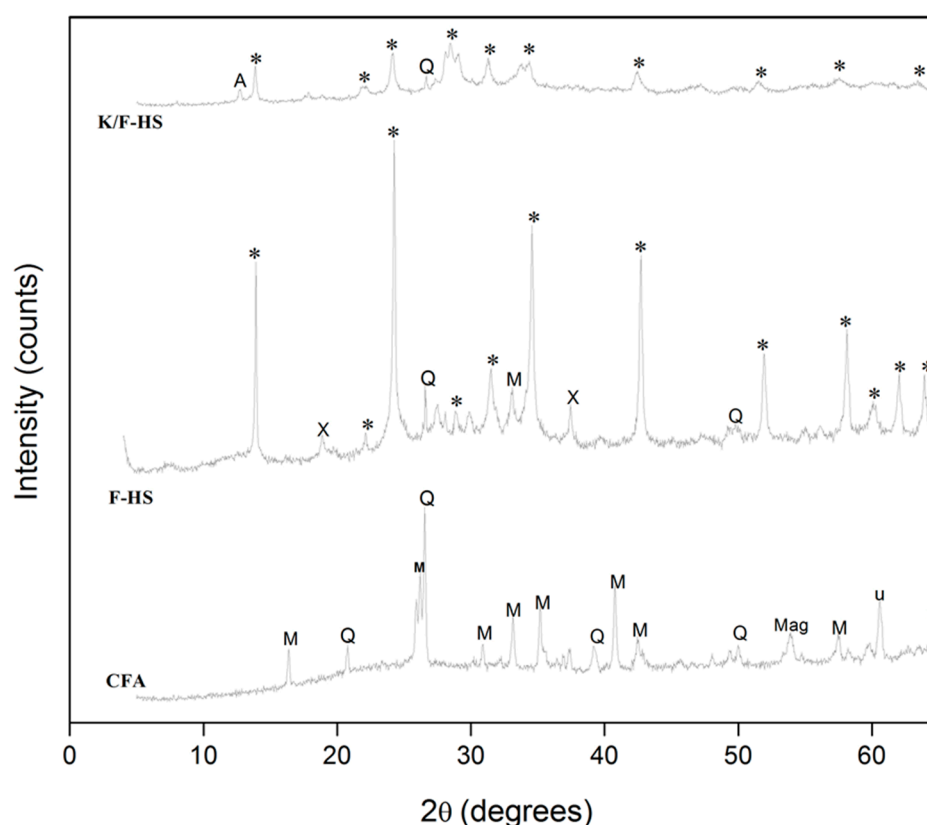

Figure 1. XRD patterns of CFA, F-HS and K/F-HS (*—hydroxy sodalite, x—zeolite X, A—zeolite A, M—mullite, Q—quartz, Mag—magnetite).

The XRD results in Figure 1 show that CFA, the feedstock material obtained from South Africa, exhibited a crystalline phase of quartz (Q) and mullite (M) in major proportion. Upon fusion-assisted hydrothermal conversion of the CFA, the XRD pattern of the obtained product F-HS exhibited the peaks of a corresponding HS zeolite phase in accordance with the standard simulated pattern of sodalite [40]. However, other mineral phases such as zeolite X and quartz were detected in F-HS samples as minor phase impurities, showing that the CFA feedstock had been almost fully converted to zeolite mineral phases during the fusion-assisted hydrothermal steps. By ion exchange modification of the sample with K^+

(K/F-HS), as described in Section 3.2.2, it was observed that the intensity of all the standard and major HS zeolite peaks at $2\theta = 14.14°$, 24.64, 35.1 and 43.36° drastically decreased. The decrease in HS crystallinity could have been due to framework instability associated with the removal of charge-balancing Na^+ cations, as well as due to the reflux conditions prescribed for ion exchange or thermal post-synthesis calcination applied, which may have been too vigorous for HS zeolite [41]. This may have also resulted in an ineffective exchange of K^+ ion as a charge balancing cation during the exchange process [17,41].

2.2. Crystal Morphology

The morphology of the produced F-HS sample shows a hexagonal-cubic crystal habit (Figure 2a). After the sample was ion-exchanged, its crystal morphology altered to a more agglomerated structure with tiny crystals (Figure 2b). Intercrystalline voids between crystals was observed, which slightly narrowed after the modification process (K/F-HS). This could be due to the high temperature calcination after ion exchange during the modification process (Figure S1 from Supplementary Materials), as well as an indication of K^+ ion deposits (Table 1) in the form of salts covering the surfaces of the catalyst [20,30].
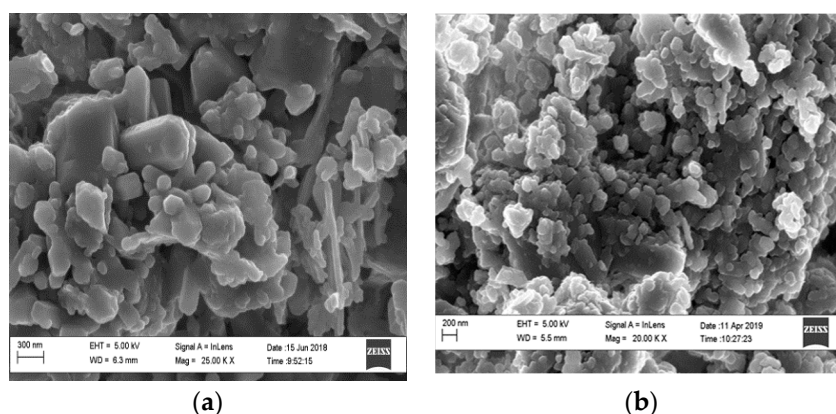

| (a) | (b) |

Figure 2. SEM image of (**a**) Fusion-assisted HS zeolite (F-HS), (**b**) Ion exchange-modified zeolite (K/F-HS).

Table 1. Elemental composition showing the effect of ion exchange-modification on produced fusion-assisted hydrothermal HS zeolite.

Sample	Element (Atomic, *w/w*%)												
	O	Al	Si	Na	Mg	K	Ca	Ti	Fe	P	Total	Si/Al	Na/Al
CFA	65.15	11.23	14.86	-	1.54	0.23	4.32	0.30	1.13	1.25	100.0	1.32	-
F-HS	65.35	12.42	14.65	11.55	0.39	-	1.18	0.29	0.57	-	100.0	1.18	0.93
K/F-HS	59.75	10.1	13.67	8.17	0.8	3.77	1.97	0.44	1.13	-	100.0	1.35	0.81

2.3. Elemental Composition

Table 1 presents the elemental composition of the samples as analysed by SEM-EDS. A significant proportion of Si (14.86%), Al (13.67%) and charge balancing Na^+ ions (11.55%) were detected in the framework of the parent HS zeolite (F-HS). The sample demonstrated a Si/Al framework ratio of 1.18 and a Na/Al ratio of 0.93. Upon ion exchange, it was observed that the percentage concentration of Si, Al and Na was reduced, with a significant increase in K^+ ion by 3.77% *w/w*. Na content declined from 11.55 (F-HS) to 8.17% (K/F-HS) *w/w* after the ion exchange modification process. This might suggest the partial exchange of Na^+ with K^+ ions due to the applied ion exchange procedure and possible enhanced catalyst basic strength [42]. Furthermore, the decrease in the proportion of major elements (Si, Al, Na) resulted in the decreased Si/Al and Na/Al ratio in the modified sample (K/F-HS). This is supported by the reduction in phase crystallinity and identity as

observed in Figure 1 [41,43]. The Si/Al ratio of a typical HS zeolite structure ranges between 0.84–1 [26,44] (Table S2); which is explained better by F-HS (Si/Al = 1.18) compared to K/F-HS (Si/Al = 1.35). The reduced Na/Al ratio observed in sample K/F-HS after ion-exchange modification is evidently due to the introduction of K ions as charge balancing cations in the framework structure [3,28,45].

2.4. Fourier-Transform Infrared

The FT-IR spectra in Figure 3 depicts the structural configuration of a fusion-assisted and ion-exchanged HS zeolite sample. From the view of the spectra, it is observed that the structural configuration describing the HS zeolite phase remained intact after modification by ion-exchange. However, the broad asymmetric stretching band of T–O–T (T = Si, Al) observed between 900–1330 cm^{-1} (± 975 cm^{-1}) in F-HS significantly narrowed, and the intensity of the two sodium carbonate (CO_3) impurity-associated bands between 1410–1480 cm^{-1}, decreased in K/F-HS. The water adsorbed band observed in the spectra of F-HS at 1650 cm^{-1} disappeared in K/F-HS. The narrowing of asymmetric bands may correspond to decreased crystallinity observed after the ion exchange [46]. The decrease of the carbonate bands shows the removal of impurities, whereas the disappearance of water adsorption bands suggests the partial removal of water from the HS zeolite structure due to the high-temperature calcination steps after the ion-exchange process (Figure S1).
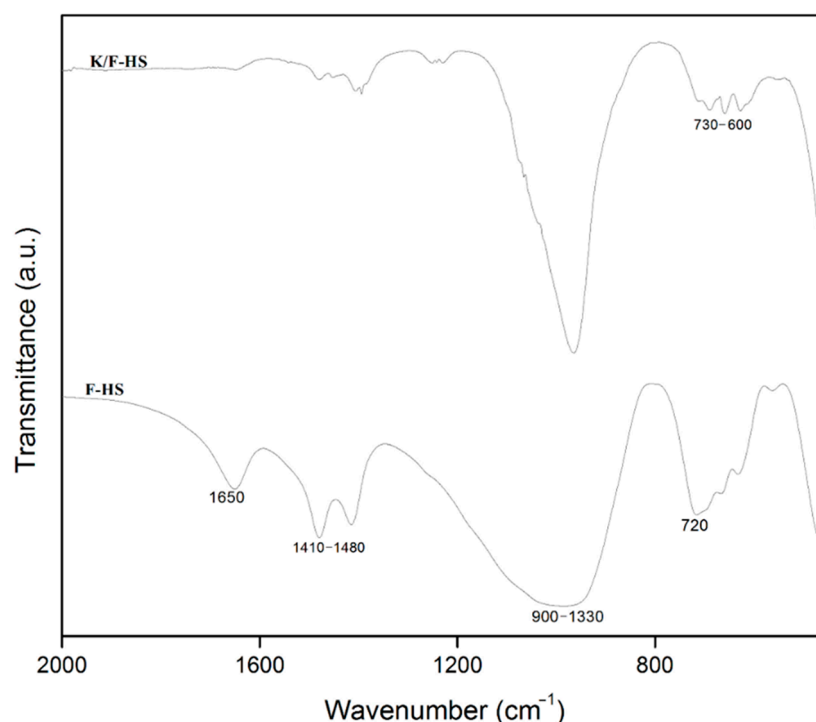

Figure 3. The FT-IR spectra illustrating the effect of ion exchange post-modification on indirect fusion HS zeolite.

2.5. Textural Properties

The textual properties of F-HS and that of the ion exchanged sample, K/F-HS, are presented in Table 2. The results show 42.2 m^2/g mesoporous area with a total surface area of 45 m^2/g (F-HS). The F-HS sample also revealed an average mesopore diameter between 12.99–15.31 nm, highlighting the mesoporous pore size distribution [47]. It may be noted in Table 2 that the total surface area of the synthesised F-HS is higher compared to HS obtained from both pure chemicals and CFA via the direct method synthesis method, as reported by Golbad et al. [44], Shipari Lapari et al. [31] and Shabani [48]. With modification by ion exchange (K/F-HS), there was a decrease in the total surface area (25.8 m^2/g),

mesoporous area (25.0 m^2/g), as well as average pore diameter range (9.5–12.20 nm). These could be attributed to surface coverage and pore blockages due to the ion exchange deposit of K$^+$ ions [25,30], owing to the larger atomic radii of K$^+$ ions compared to Na$^+$ ions in the parent F-HS [49]. The high temperature calcination and the apparently high reflux conditions prescribed for ion exchange [25,50] over HS using a KOH alkali source in this work (Section 3.2.2), might also justify the above results. The evidence of decreased surface area and pore volumes due to the coverage of K$^+$ ions and the above-mentioned conditions also can indicate poor exchange between the Na$^+$ ions initially present in the parent F-HS structure and K$^+$ ions in the modification process. The lower resultant mesoporous area in K/F-HS suggests pore blockage and a decrease in mesoporous characteristics after ion exchange.

Table 2. Textual properties of parent and ion exchange-modified HS.

Synthesis Method	Sample	Source	Surface Area (m^2/g)			Reference
			Total [a]	Meso. [b]	Micro. [b]	
Fusion	F-HS	CFA	45	42.2	2.7	This study
Direct	HS	CFA	13.2	12.6	0.6	Shabani [48]
Conventional direct	HS	Pure chemicals	43.6	-	9.6	Golbad, Khoshnoud and Abu-Zahra [44]
Conventional direct	HS	Pure chemicals	11	-	-	Shirani Lapari, Ramli and Triwahyono [31]
Ion exchange	K/F-HS		25.8	25	0.8	This study

[a] Obtained by BET equation/method at p/p$_0$ = 0.99. [b] Measured by t-plot which defines pores in the sample of 2–50 nm (mesopore) and <2 nm (micro) in width [47].

Pore Distribution and Isotherm Curves of Produced Catalysts

The pore size distribution curve (Figure 4) reveals that the parent F-HS zeolite contained mesopores of 4 nm average diameter. The modified sample, K/F-HS, shows more intense and broader peaks, with pore sizes distributed around 3–5 nm (Figure 4). The modified sample further shows a broader pore size distribution between 15 and 30 nm (~24 nm), which could imply larger mesopores with lower external surface area associated with more diffusive characteristics (less diffusion constraints) compared to the parent zeolite [33,51].

Furthermore, the N$_2$ adsorption isotherm curves of the samples are presented in Figure 5. Both samples show a typical isotherm representing a characteristic type III of Langmuir adsorption as classified by IUPAC [52]. The isotherm curves of the two samples commonly show a micropore filling in the region p/p^o below 0.4, with a small adsorption type H$_3$ hysteresis loop in the range of p/p^o > 0.45. It is suggested by Sotomayor et al. [47] and Thommes et al. [52] that this loop indicates mesoporosity that enhanced capillary condensation of the adsorbed nitrogen, and the loop is associated with a shallow micropore area. The narrower hysteresis shown by the modified sample (K/F-HS), signifies lower mesoporosity than the parent zeolite (F-HS), which was affirmed by the BET results in Table 2.

2.6. Biodiesel Production over CFA-Synthesised and Modified HS Zeolite

The obtained fusion F-HS zeolite and ion-exchanged zeolite (K/F-HS) was used for transesterifying waste-derived BSF maggot oil. Figure 6 shows a high biodiesel yield of 84.10% with a considerable FAME content of 64.50% over the synthesised F-HS catalyst. With a small micropore size (2.8 Å) (Table S1), HS micropores are too constrained to allow the diffusion of biodiesel into micropores, thus the non-microporous surface area (mesopores and macropores) in the nanometre size were readily accessible and allowed the rapid conversion of maggot oil to biodiesel (Table 2). Using ion exchange modified K/F-HS resulted in a biodiesel yield of 83.70% and a considerably decreased FAME content of

51.50%. The slight decline in the yield obtained using the modified K/F-HS sample could be due to decreased total surface area (Table 2). This could be explained by lower reactant (oil-methanol) surface interaction in the process [3,20]. The decrease in FAME content using K/F-HS could also be attributed to possible poor diffusive characteristics offered by the modified sample due to smaller average pore size (Table S2) and pore blockages, as well as possible decreased acidity of the sample [28,53]. Thus, there is a high possibility that the reaction has occurred only on the external mesopore surface area (non-micropore areas) of the K/F-HS, compared to the extent of reaction that occurred over the parent F-HS zeolite [25,36,54]. The FAME content suggests good quality biodiesel obtained over the catalyst F-HS [55], compared to the quality of biodiesel obtained using K/F-HS. Nevertheless, both biodiesel samples obtained over the catalysts (Table 3) resulted in fuel quality properties that comply with the ASTMD6751 and EN14214 standard specifications [56]. It should also be noted that the fusion-assisted synthesis method for HS zeolite was associated with better catalytic performance on the basis of textural properties (Table 2) [51]. The method also on this basis, resulted in better yield and quality biodiesel compared to the direct hydrothermal method synthesis of the catalyst [48].
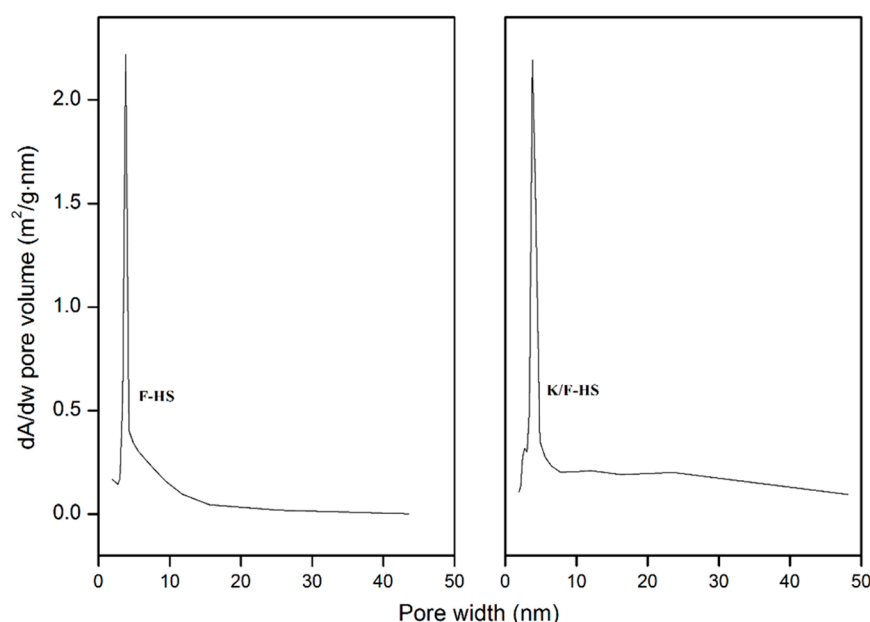

Figure 4. Pore size distribution of fusion-assisted hydrothermal F-HS and ion exchange-modified K/F-HS zeolite.

Table 3. Properties of biodiesel derived from maggot oil using the fusion-synthesised and ion exchange modified HS zeolite catalyst.

Biodiesel Properties	Catalyst		B-Standard [a]
	F-HS	**K/F-HS**	**ENS [b]/ASTM [c]**
Acid value (mg KOH/g)	0.53	0.74	0.5/0.8 Max
Saponification value (mg KOH/g)	147.87	145.43	-
Ester content [d] (% m/m)	64.95	51.5	96.5
Iodine value (g of I_2/100 g)	65.01	61.4	/120–130
Density at 40 °C (g/mL)	0.877	0.893	0.86–0.90
Kinematics viscosity at 40 °C (mm^2/s)	5.16	4.68	3.5–5.0/1.9–6.0
Refractive index	1.4455	1.4435	/1.479
Cetane number	36.63	36.66	51/47

[a] Biodiesel Standard Specifications; [b] ENS14214 (European) and [c] ASTMD6751 (American); [d] Obtained from GC characterisation of biodiesel samples, also referred to as FAME content.
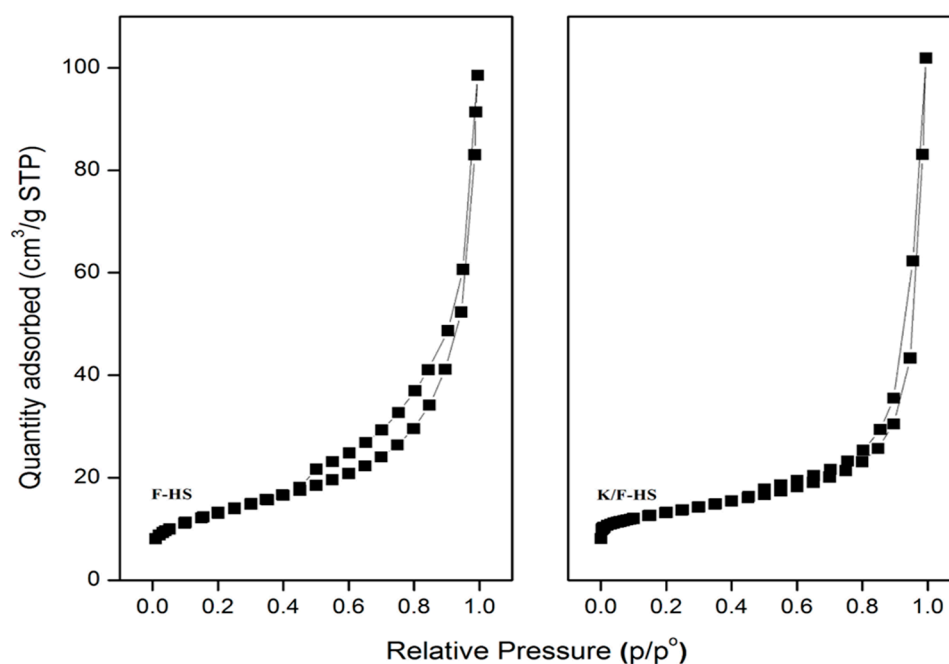
Figure 5. N_2 adsorption-desorption isotherms of fusion hydrothermal F-HS zeolite and ion exchange-modified K/F-HS zeolite.
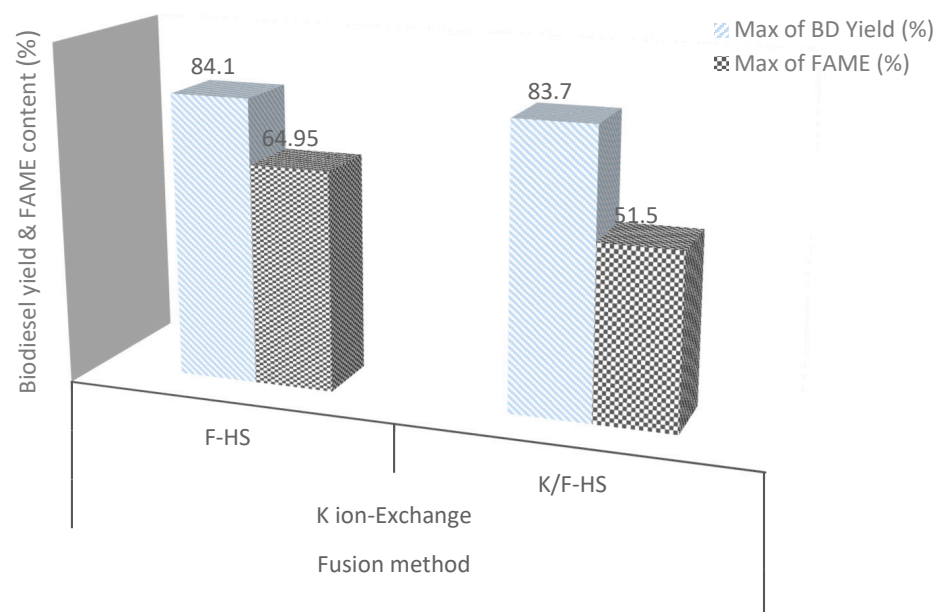

Figure 6. Yield and FAME content of biodiesel derived over fusion hydrothermal and ion-exchanged HS zeolite (FAME content equivalent to ester content).

Table 4 reports on the performance of F-HS zeolite and ion-exchanged K/F-HS zeolite compared to the performance of the counterpart zeolites reported in the literature for biodiesel production. The results herein reveal that both the parent F-HS and ion exchange K/F-HS resulted in better biodiesel yield performance than all zeolites reported in the literature [25,30]. In addition to biodiesel yield, these results are novel due to the properties of biodiesel obtained in each case, which attest to the outstanding performance of the HS zeolite catalyst in biodiesel production.

Table 4. The performance of fly ash-derived and ion exchange-modified HS zeolite in biodiesel production compare to the literature's counterpart HS zeolite catalysts.

Biodiesel Feedstock	Zeolite Catalyst		Ion Exchange Post-Synthesis	Biodiesel		Reference
	Type (Source)	Hydrothermal Synthesis Method		Yield (%)	Properties	
WCO	ZSM-5 (* pure chem. reagents)	Direct	$\times$ $\sqrt{}$(NH$_4$Cl)	-	-	Fawaz, Salam, S. Rigolet and Daou [24]
Oleic acid	ZSM-5, ZRP-5, Beta (* pure chem. reagents)	-	$\times$ $\sqrt{}$(NH$_4$Cl)	-	-	Sun, Lu, Ma, Han, Fu and Ding [21]
Mustard oil	Na-X (CFA)	Fusion	$\times$ $\sqrt{}$(CH$_3$COOK)	41.90 53.7	- -	Volli and Purkait [25]
Sunflower oil	Na-X (CFA)	Fusion	$\times$ $\sqrt{}$(CH$_3$COOK)	56 83.52	- -	Babajide, Musyoka, Petrik and Ameer [30]
WCO	HS (* pure chem. reagents)	Direct	$\times$	-	-	Makgaba and Daramola [36]
* BSF oil	HS (CFA)	Fusion	$\times$ $\sqrt{}$(KOH)	84.10 83.70	$\sqrt{}\sqrt{}$ $\sqrt{}\sqrt{}$	This study

* Pure chem. reagents: pure chemical reagents, commercially supplied. $\times$ unmodified zeolite; $\sqrt{}$**(CH₃COOK) or KOH**: ion exchange-modified using either CH$_3$COOK (potassium acetate) or KOH (hydroxide). (-) not conducted/reported; $\sqrt{}\sqrt{}$ Biodiesel analysis (properties) conducted/reported. * BSF oil: waste-derived maggot oil feedstock from black solider fly (BSF).

2.7. Techno-Economic and Environmental Impact of Hydroxyl Sodalite (F-HS) as a Heterogeneous Catalyst Compared to a Conventional Homogenous Catalyst in Biodiesel Production

Further evaluation of the performance of HS zeolite as a heterogeneous catalyst in biodiesel production was conducted on the basis of economic and environmental impact, vis-à-vis the conventional homogenous catalyst, sodium hydroxide, in the transesterification of BSF oil (Table 5 and Table S4). Introducing HS zeolite (F-HS) as heterogeneous catalyst as substitute for the conventional NaOH catalyst resulted in a decrease in cost and mass input of feedstock oil by 17% of the cost of feedstock required using NaOH conventional catalyst) per kg of biodiesel produced (Table S4). This is mostly due to the higher biodiesel yield obtained using the F-HS zeolite (84.10%) compared to the homogeneous NaOH catalyst at fixed conditions using the same feedstock oil. Furthermore, the heterogeneous catalyst F-HS, in terms of catalyst cost, was about four times more costly than the conventional NaOH homogeneous catalyst per kg of biodiesel produced in each case (i.e., $1.39 vs. $0.36/kg biodiesel) at fixed conditions (Table S4). This might imply that the use of HS zeolite was less profitable (cost-benefit) in terms of catalyst cost compared to the cost of the NaOH catalyst. However, it should be noted that the HS heterogeneous catalyst was recoverable and has the possibility of being reused for several biodiesel production cycles, unlike NaOH, which gets spent by excess washing after use [5]. Thus, this might compensate for the cost of HS in terms of catalyst cost in biodiesel production.

The environmental benefits of employing an HS zeolite heterogeneous catalyst (F-HS) as opposed to an NaOH conventional homogeneous catalyst highlights that HS zeolite obtainable from waste coal fly ash minimizes pollution in serving as a disposal management strategy of the solid waste from coal power stations (Table 5). The use of heterogeneous HS is also associated with less wastewater generation (Table S4) as opposed to the alkali wastewater disposed of during the washing of biodiesel produced in the presence of the homogeneous NaOH. The cost of the effluent treatment was estimated to be lower than that discharged from the NaOH-catalysed biodiesel production process.

Table 5. Economic and environmental benefit/impact of HS heterogeneous catalyst compared to NaOH homogeneous-transesterification in biodiesel production.

* Catalysed-Transesterification	Techno-Economic Impact	Enviromental Impact	Reference
NaOH homogeneous-	• High production cost associated with BD water washing and purification steps; and possible treatment of excess effluent	• Disposal of excess wastewater generation from BD purification and possible pollution: 20% excess wastewater compared to HS-heterogeneous catalyst (Table S4)	• Mansir, et al. [57] • Shabani, Babajide and Oyekola [6]
HS-catalysed	• Reduced BD production cost for catalyst derived from waste and low-cost coal fly ash material (waste beneficiation)	• Environmental benefit (pollution minimization) associated with appropriate disposal of CFA (as zeolite feedstock)	• Zielke-Olivier and Vermeulen [19] • Boycheva, et al. [58]
	• Reduced cost and volume of feedstock oil per kg of BD produced: ~17% cost reduction (Table S4)	-	• This work • Okechukwu, Joseph, Nonso and Kenechi [5]
	• Reduced cost (based on volume) of process water requirement for BD purification: ~20% cost reduction/kg of BD (Figure S3) • Reduced cost (based on volume) of possible effluent (wastewater) treatment from BD purification: ~19.8% cost reduction/kg of BD (Table S4)	• Reduced wastewater generation (volume) and associated disposal implications from BD purification step: 19.8% reduced wastewater *volume*/kg BD (Table S4)	• This work
	• High yield biodiesel product compared to NaOH homogenous in previous work: 84.10% versus 69.93%	-	• This work • Shabani, Babajide and Oyekola [6]
	• Was recovered in this work; has high possibility of reuse and regeneration	• Minimises disposal requrement and impact	• This work • Faria, et al. [59]; • Saifuddin, et al. [60]; • Leung, et al. [61]

BD: biodiesel. * BSF oil was used as fixed feedstock for comparison of cases between the two catalysts.

3. Materials and Methods

3.1. Materials

Coal fly ash, the starting material for zeolite synthesis, was obtained in the Mpumalanga province of South Africa. The following reagents were used as purchased: sodium hydroxide (NaOH) pellets (98% grade—Kimix Chemical, Cape Town, South Africa), potassium hydroxide (KOH) pellets (85% grade—Sigma Aldrich, Johannesburg, South Africa), methanol (99.50% grade—Sigma Aldrich) and sodium sulphate (Na_2SO_4) dehydrant (Sigma Aldrich). The BSF maggot oil feedstock for biodiesel transesterification tests was obtained from Inseco (AgriProtein) Ltd. (Cape Town, South Africa).

3.2. Catalyst Preparation and Ion Exchange Modification

Figure 7 illustrates the process flow of the fusion-assisted hydrothermal synthesis, the post-modification of the catalyst, the characterization and the application of the catalysts in transesterification reaction for biodiesel (BD) production from BSF oil.
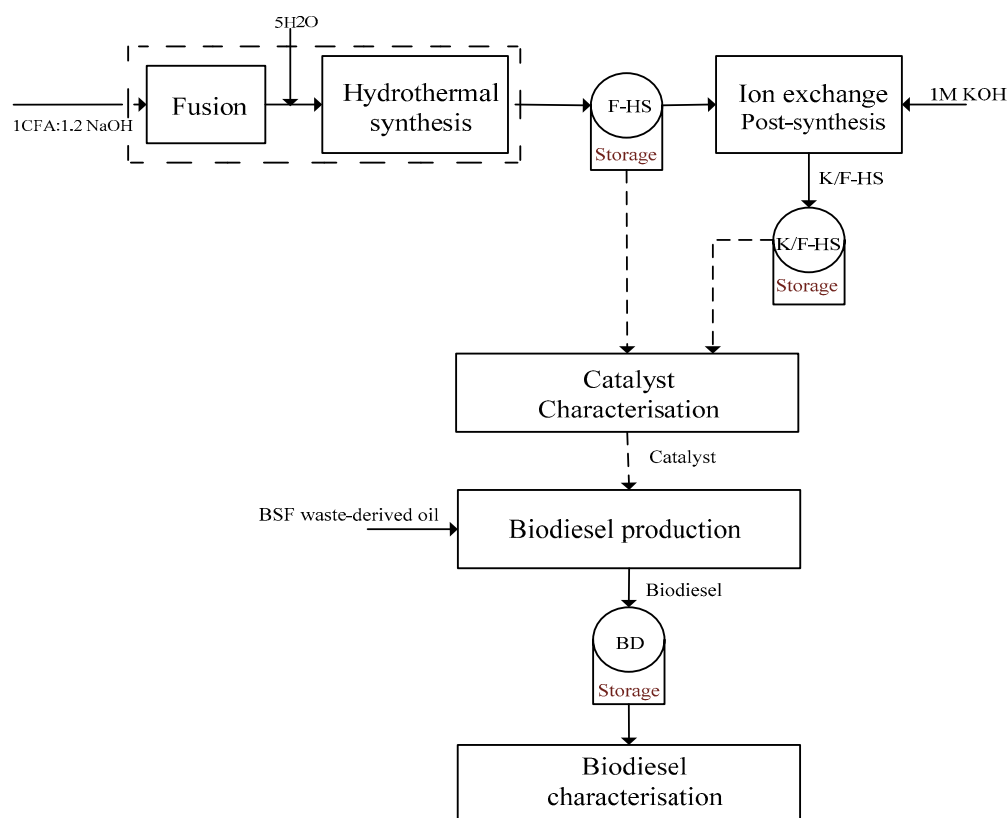
Figure 7. Schematic diagram illustrating the experimental processes (detailed process for IE in Figure S1, for BD in Figure S2).

3.2.1. Fusion-Assisted Hydrothermal Synthesis

The mass-mass ratio of 1:1.2 coal fly ash-NaOH mixture was crushed and then fused in a furnace at a temperature of 550 °C for 1.5 h. Thereafter, 50 mL of deionized water was added to the fused sample in a 100 mL Teflon-lined autoclave for hydrothermal reaction at 100 °C for 144 h. The obtained solid product from the reaction was filtered, washed, and dried overnight. The final product (with code name F-HS) was characterized using XRD, EDS, SEM, FT-IR and BET-BJH.

3.2.2. Post-Synthesis Ion-Exchange Modification

The modification of the obtained F-HS catalyst by ion-exchange using KOH as an alkali source was conducted according to the procedure previously described [25,50] (Figure S1). 1 g of the prepared catalyst (F-HS) was mixed with 1 M KOH solution in a mass ratio of 1:10 (Figure S1 and Figure 7). The slurry mixture was ion-exchanged by reflux at 60 °C for 24 h using a stirring speed of 800 rpm. The modified product was filtered, washed, and dried overnight at 120 °C. This was followed by calcination of the dried solid product in a muffle furnace at 550 °C for 1.5 h. The final modified solid product was assigned the code name K/F-HS.

3.2.3. Activity Tests of Synthesized Catalysts in Biodiesel Production from BSF Oil

The procedure for transesterification of waste-derived BSF oil for biodiesel production using the synthesized catalysts is schematically presented in Figure 7. The detailed procedure is presented in Figure S2 (Supplementary Materials).

The batch transesterification reaction was achieved in a round-bottom flask over a hotplate heating source whilst stirring at 800 rpm at a temperature of 60 °C for 1.5 h. A fixed catalyst weight of 1.5% to the weight of the oil was used, as was a methanol (MeOH) amount equivalent to MeOH-to-oil molar ratio of 15:1. The obtained product mixture containing biodiesel was centrifuged for phase and catalyst separation. The biodiesel containing-phase

was washed thoroughly with deionized water, dried by heating and addition of anhydrous sodium sulphate, cooled, weighed, and stored prior to characterization.

The yield of biodiesel obtained, in the case of each catalyst used, was determined using Equation (1).

$$Yield\ of\ biodiesel,\ (\%) = \frac{mass\ of\ biodiesel\ obtained}{mass\ of\ oil\ feedstock} \times 100 \qquad (1)$$

3.3. Catalyst and Biodiesel Sample Characterisation

A sample characterization was conducted on both catalysts produced and derived-biodiesel samples. The catalysts were characterized using X-ray diffraction (XRD), energy-dispersive X-ray spectroscopy (EDS), Fourier-transform infrared (FT-IR) and Brunauer–Emmett–Teller (BET) coupled with the Barret-Joyner-Halenda (BJH) analysis, with detailed description in Table 6. The XRD patterns of the obtained products were assigned according to the standard diffraction pattern of the sodalite zeolite structure obtained from the International Zeolite Association's (IZA) database [40].

Table 6. Characterization of catalyst and biodiesel samples (instruments, operating conditions).

Characterisation Catalyst	Instrument Model	Detector	Operating Conditions
XRD	Bruker AXS (Bruker, Billerica, MA, USA)	LynxEye detector	Cu-Kα radiation (ń;Kα1 = 1.5406 Å), 40 kV, 40 mA.
EDS-SEM	ZeiSS Gemini Auriga (high mag, Carl Zeiss AG, Jena, Germany)	CDU-lad detector	25 kV
FT-IR	Perkin Elmer 100 FT-IR (Perkin Elmer, Waltham, MA, USA	-	Sample configuration data set-range (450–2000 cm^{-1})
BET-BJH	3Flex version 5.00, serial # 990 (Micromeritics, Norcross, GA, USA)	-	Adsorption-desorption isotherms (77.6 K, 5 h)
** Biodiesel	Instrument/analytical method	-	Reference
Density	Density meter (DMA, Anton Paar)	-	Anastopoulos, et al. [62]
Viscosity at 40 °C	Rheometer (* DHR) (ISO 3104)	-	AMSEC [63]
Acid value	Titrimetric methods (ISO 1242)	-	Lucas [64]
Saponification	Titrimetric method (AOCS CD3)	-	Babajide [65]
Iodine value	Wij's method (EN 14111)	-	Japir, et al. [66]
FAME/ester	* GC-FID (HP88GC) (EN 14103)	Polar capillary column	Anastopoulos, Zannikou, Stournas and Kalligeros [62]
Refractive index, *n*	Refractometer (#PA203 Misco)	-	-
Cetane value, ∅*i*	Empirical correlation	-	Ramírez-Verduzco, et al. [67]

* DHR—Discovery HR-1 hybrid. * GC-FID machine was pre-calibrated for FAME analysis. ** BSF oil (commercially known as maggot oil) was characterised similarly as the biodiesel samples, with results reported and referenced from our previous study [6,68].

The biodiesel samples obtained (Figure S2) were characterized in accordance with the American Society for Testing and Materials (ASTMD6751) and the European normalization (EN14214) standards. The characterization techniques, used instruments (analytical methods) and operating conditions are presented in Table 5.

4. Conclusions

Hydroxy sodalite zeolite synthesised using coal fly ash waste-feedstock was successfully obtained via fusion-assisted hydrothermal synthesis. The zeolite possessed high crystalline characteristics, high mesoporous characteristics (average pore diameter range 12.99–15.31 nm) and a considerable total surface area of 45 m^2/g. With a small micropore size (2.8 Å), HS micropores are too constrained to allow the diffusion of biodiesel into micropores; thus the high mesopore external surface area allowed for the rapid conversion of BSF maggot oil to biodiesel. The post-synthesis modification by ion exchange of the

catalyst with KOH adversely affected the crystallinity and textural properties of the zeolite due to poor K$^+$ exchange. The F-HS zeolite sample proved to be highly active in biodiesel production from waste BSF maggot oil, leading to a high biodiesel yield of 84.10% and considerable quality with 64.95% FAME content. The modified sample (K/F-HS) presented reasonable activity for biodiesel production, with substandard 51.50% FAME content as compared to the parent F-HS zeolite. Thus, it was not necessary or favourable to conduct the post-modification of HS zeolite by ion exchange for biodiesel production using a KOH alkali source at high reflux conditions (temperature, agitation rate) nor to utilize a calcination step inclusive thereafter, as applied in this work. The synthesised F-HS also produced better biodiesel yield, at a lower cost of feedstock oil (~20% reduced cost per kg of biodiesel produced), and had better environmental implications of its use compared to the use of the NaOH homogenous catalyst for biodiesel production. On the basis of textural properties associated with better catalytic performance, the fusion-assisted hydrothermal synthesis of HS zeolite is deemed worthwhile for better yield and quality biodiesel in comparison to the catalyst obtained via the direct method synthesis. Thus, it is recommended to investigate whether high yield or quality in both zeolite and biodiesel products is offset by the greater energy requirement of the fusion-assisted protocol. This study has shown the valorization of waste-coal fly ash and waste-derived BSF oil feedstock into mesoporous HS zeolite catalyst and biodiesel, respectively, revealing the potential of the low-cost feedstocks to minimize biodiesel production costs and ensure sustainable production.

References

1. Naylor, R.L.; Higgins, M.M. The rise in global biodiesel production: Implications for food security. *Glob. Food Secur.* **2017**, *16*, 75–84. [CrossRef]
2. Gonfa Keneni, Y.; Mario Marchetti, J. Oil extraction from plant seeds for biodiesel production. *AIMS Energy* **2017**, *5*, 316–340. [CrossRef]
3. Lam, M.K.; Lee, K.T.; Mohamed, A.R. Homogeneous, heterogeneous and enzymatic catalysis for transesterification of high free fatty acid oil (waste cooking oil) to biodiesel: A review. *Biotechnol. Adv.* **2010**, *28*, 500–518. [CrossRef] [PubMed]
4. You, Y.-D.; Shie, J.-L.; Chang, C.-Y.; Huang, S.-H.; Pai, C.-Y.; Yu, Y.-H.; Chang, C.H. Economic cost analysis of biodiesel production: Case in soybean oil. *Energy Fuels* **2008**, *22*, 182–189. [CrossRef]
5. Okechukwu, O.D.; Joseph, E.; Nonso, U.C.; Kenechi, N.-O. Improving heterogeneous catalysis for biodiesel production process. *Clean. Chem. Eng.* **2022**, *3*, 100038. [CrossRef]
6. Shabani, J.; Babajide, O.; Oyekola, O. An Investigation into the Potential of Maggot Oil as a Feedstock for Biodiesel Production. In *Valorization of Biomass to Value-Added Commodities*; Springer: Berlin/Heidelberg, Germany, 2020; pp. 285–301.
7. Wang, C.; Qian, L.; Wang, W.; Wang, T.; Deng, Z.; Yang, F.; Xiong, J.; Feng, W. Exploring the potential of lipids from black soldier fly: New paradigm for biodiesel production (I). *Renew. Energy* **2017**, *111*, 749–756. [CrossRef]
8. Leong, S.Y.; Kutty, S.R.M.; Malakahmad, A.; Tan, C.K. Feasibility study of biodiesel production using lipids of Hermetia illucens larva fed with organic waste. *Waste Manag.* **2016**, *47*, 84–90. [CrossRef]
9. Oonincx, D.; Van Huis, A.; Van Loon, J.J.A. Nutrient utilisation by black soldier flies fed with chicken, pig, or cow manure. *J. Insects Food Feed.* **2015**, *1*, 131–139. [CrossRef]
10. Hajjari, M.; Tabatabaei, M.; Aghbashlo, M.; Ghanavati, H. A review on the prospects of sustainable biodiesel production: A global scenario with an emphasis on waste-oil biodiesel utilization. *Renew. Sustain. Energy Rev.* **2017**, *72*, 445–464. [CrossRef]
11. Inseco. Our Products. 2022. Available online: https://store.inseco.co.za/product/entooil/ (accessed on 20 September 2022).
12. Ecosystem. Our product. 2010. Available online: http://www.eco-system.com/products.php (accessed on 15 June 2022).
13. Dwivedi, A.; Jain, M.K. Fly ash—Waste management and overview: A Review. *Recent Res. Sci. Technol.* **2014**, *6*, 30–35.
14. Heidrich, C.; Feuerborn, H.-J.; Weir, A. Coal combustion products: A global perspective. In Proceedings of the World of Coal Ash Conference, Covington, KY, USA, 16–19 May 2022; 2022; p. 25.
15. Brassell, J.P. Investigation of some Scale-up Conditions on the Synthesis of Faujasite Zeolites from South African Coal Fly Ash. Ph.D. Thesis, Cape Peninsula University of Technology, Cape Town, South Africa, 2017.
16. Murayama, N.; Yamamoto, H.; Shibata, J. Mechanism of zeolite synthesis from coal fly ash by alkali hydrothermal reaction. *Int. J. Miner. Process.* **2002**, *64*, 1–17. [CrossRef]
17. Querol, X.; Moreno, N.; Umaña, J.t.; Alastuey, A.; Hernández, E.; Lopez-Soler, A.; Plana, F. Synthesis of zeolites from coal fly ash: An overview. *Int. J. Coal Geol.* **2002**, *50*, 413–423. [CrossRef]
18. Vilakazi, A.Q.; Ndlovu, S.; Chipise, L.; Shemi, A. The recycling of coal fly ash: A review on sustainable developments and economic considerations. *Sustainability* **2022**, *14*, 1958. [CrossRef]
19. Zielke-Olivier, J.; Vermeulen, D. Fine Ash Leaching in Tailings Dams–An Impact on the Underlying Aquifers? *Proc. IMWA* **2016**, 353–360.
20. Chouhan, A.P.S.; Sarma, A.K. Modern heterogeneous catalysts for biodiesel production: A comprehensive review. *Renew. Sustain. Energy Rev.* **2011**, *15*, 4378–4399. [CrossRef]
21. Sun, K.; Lu, J.; Ma, L.; Han, Y.; Fu, Z.; Ding, J. A comparative study on the catalytic performance of different types of zeolites for biodiesel production. *Fuel* **2015**, *158*, 848–854. [CrossRef]
22. Suppes, G.J.; Dasari, M.A.; Doskocil, E.J.; Mankidy, P.J.; Goff, M.J. Transesterification of soybean oil with zeolite and metal catalysts. *Appl. Catal. A: Gen.* **2004**, *257*, 213–223. [CrossRef]
23. Sivasamy, A.; Cheah, K.Y.; Fornasiero, P.; Kemausuor, F.; Zinoviev, S.; Miertus, S. Catalytic Applications in the Production of Biodiesel from Vegetable Oils. *ChemSusChem* **2009**, *2*, 278–300. [CrossRef]
24. Fawaz, E.G.; Salam, D.A.; Rigolet, S.S.; Daou, T.J. Hierarchical zeolites as catalysts for biodiesel production from waste frying oils to overcome mass transfer limitations. *Molecules* **2021**, *26*, 4879. [CrossRef]
25. Volli, V.; Purkait, M.K. Selective preparation of zeolite X and A from flyash and its use as catalyst for biodiesel production. *J. Hazard. Mater.* **2015**, *297*, 101–111. [CrossRef]
26. Nanganoa, L.T.; Mbadcam, K.J.; Kang, S. Synthesis of Hydroxy-sodalite from Fine Fractions of Sandy Clay Loam Soil (Natural Aluminosilicate). *Int. J. Chem. Tech. Res.* **2016**, *9*, 725–732.
27. Musyoka, N.M.; Petrik, L.F.; Balfour, G.; Gitari, W.M.; Hums, E. Synthesis of hydroxy sodalite from coal fly ash using waste industrial brine solution. *J. Environ. Sci. Health Part A* **2011**, *46*, 1699–1707. [CrossRef] [PubMed]
28. Ferreira Madeira, F.; Ben Tayeb, K.; Pinard, L.; Vezin, H.; Maury, S.; Cadran, N. Ethanol transformation into hydrocarbons on ZSM-5 zeolites: Influence of Si/Al ratio on catalytic performances and deactivation rate. Study of the radical species role. *Appl. Catal. A Gen.* **2012**, *443–444*, 171–180. [CrossRef]
29. Xie, W.; Huang, X.; Li, H. Soybean oil methyl esters preparation using NaX zeolites loaded with KOH as a heterogeneous catalyst. *Bioresour. Technol.* **2007**, *98*, 936–939. [CrossRef]
30. Babajide, O.; Musyoka, N.; Petrik, L.; Ameer, F. Novel zeolite Na-X synthesized from fly ash as a heterogeneous catalyst in biodiesel production. *Catal. Today* **2012**, *190*, 54–60. [CrossRef]

31. Shirani Lapari, S.; Ramli, Z.; Triwahyono, S. Effect of Different Templates on the Synthesis of Mesoporous Sodalite. *J. Chem.* **2015**, *2015*, 272613. [CrossRef]

32. Bukhari, S.S.; Behin, J.; Kazemian, H.; Rohani, S. A comparative study using direct hydrothermal and indirect fusion methods to produce zeolites from coal fly ash utilizing single-mode microwave energy. *J. Mater. Sci.* **2014**, *49*, 8261–8271. [CrossRef]

33. Viswanadham, N.; Saxena, S.K.; Kumar, J.; Sreenivasulu, P.; Nandan, D. Catalytic performance of nano crystalline H-ZSM-5 in ethanol to gasoline (ETG) reaction. *Fuel* **2012**, *95*, 298–304. [CrossRef]

34. Hollman, G.; Steenbruggen, G.; Janssen-Jurkovičová, M. A two-step process for the synthesis of zeolites from coal fly ash. *Fuel* **1999**, *78*, 1225–1230. [CrossRef]

35. Mezni, M.; Hamzaoui, A.; Hamdi, N.; Srasra, E. Synthesis of zeolites from the low-grade Tunisian natural illite by two different methods. *Appl. Clay Sci.* **2011**, *52*, 209–218. [CrossRef]

36. Makgaba, C.P.; Daramola, M.O. Transesterification of Waste Cooking Oil to Biodiesel over Calcined Hydroxy Sodalite (HS) Catalyst: A preliminary investigation. In Proceedings of the 2015 International Conference on Sustainable Energy and Environmental Engineering (SEEE 2015), Bangkok, Thailand, 25–26 October 2015.

37. Aniokete, T.; Ozonoh, M.; Daramola, M.O. Synthesis of pure and high surface area sodalite catalyst from waste industrial brine and coal fly ash for conversion of waste cooking oil (WCO) to biodiesel. *Int. J. Renew. Energy Res. (IJRER)* **2019**, *9*, 1924–1937.

38. Xu, M.; Mukarakate, C.; Robichaud, D.J.; Nimlos, M.R.; Richards, R.M.; Trewyn, B.G. Elucidating zeolite deactivation mechanisms during biomass catalytic fast pyrolysis from model reactions and zeolite syntheses. *Top. Catal.* **2016**, *59*, 73–85. [CrossRef]

39. Luo, J.; Zhang, H.; Yang, J. Hydrothermal Synthesis of Sodalite on Alkali-Activated Coal Fly Ash for Removal of Lead Ions. *Procedia Environ. Sci.* **2016**, *31*, 605–614. [CrossRef]

40. Treacy, M.M.; Higgins, J.B. *Collection of Simulated XRD Powder Patterns for Zeolites Fifth Revised Edition*, 5th ed.; Elsevier: Amsterdam, Netherlands, 2007.

41. Rayalu, S.; Meshram, S.; Hasan, M. Highly crystalline faujasitic zeolites from flyash. *J. Hazard. Mater.* **2000**, *77*, 123–131. [CrossRef]

42. Suppes, G.; Bockwinkel, K.; Lucas, S.; Botts, J.; Mason, M.; Heppert, J. Calcium carbonate catalyzed alcoholysis of fats and oils. *J. Am. Oil Chem. Soc.* **2001**, *78*, 139–146. [CrossRef]

43. Rios, C.A.; Williams, C.D.; Fullen, M.A. Nucleation and growth history of zeolite LTA synthesized from kaolinite by two different methods. *Appl. Clay Sci.* **2009**, *42*, 446–454. [CrossRef]

44. Golbad, S.; Khoshnoud, P.; Abu-Zahra, N. Hydrothermal synthesis of hydroxy sodalite from fly ash for the removal of lead ions from water. *Int. J. Environ. Sci. Technol.* **2017**, *14*, 135–142. [CrossRef]

45. Endalew, A.K.; Kiros, Y.; Zanzi, R. Inorganic heterogeneous catalysts for biodiesel production from vegetable oils. *Biomass Bioenergy* **2011**, *35*, 3787–3809. [CrossRef]

46. Buhl, J.-C.; Schuster, K.; Robben, L. Nanocrystalline sodalite grown from superalkaline NaCl bearing gels at low temperature (333 K) and the influence of TEA on crystallization process. *Microporous Mesoporous Mater.* **2011**, *142*, 666–671. [CrossRef]

47. Sotomayor, F.J.; Cychosz, K.A.; Thommes, M. Characterization of micro/mesoporous materials by physisorption: Concepts and case studies. *Acc. Mater. Surf. Res.* **2018**, *3*, 36–37.

48. Shabani, J.M. Synthesis of Fly Ash-Based Zeolites for Use as Catalysts in the Transesterification of Waste-Derived Maggot Oil for Biodiesel Production. Ph.D. Thesis, Cape Peninsula University of Technology, Cape Town, South Africa, 2021.

49. Nathan. Atomic Radius of Elements. 2022. Available online: https://www.breakingatom.com/learn-the-periodic-table/atomic-radius-of-elements (accessed on 10 July 2022).

50. Volli, V. Preparation and Characterization of Flyash Based Catalyst for Transesterification of Mustard Oil. Ph.D. Thesis, Indian Institute of Technology Guwahati, Guwahati, India, 2015.

51. Weitkamp, J. Zeolites and catalysis. *Solid State Ion.* **2000**, *131*, 175–188. [CrossRef]

52. Thommes, M.; Kaneko, K.; Neimark, A.V.; Olivier, J.P.; Rodriguez-Reinoso, F.; Rouquerol, J.; Sing, K.S. Physisorption of gases, with special reference to the evaluation of surface area and pore size distribution (IUPAC Technical Report). *Pure Appl. Chem.* **2015**, *87*, 1051–1069. [CrossRef]

53. Dehkhoda, A.M. Developing Biochar-Based Catalyst for Biodiesel Production. Master's thesis, University of British Columbia, Vancouver, BC, Canada, 2010.

54. Endalew, A.K.; Kiros, Y.; Zanzi, R. Heterogeneous catalysis for biodiesel production from Jatropha curcas oil (JCO). *Energy* **2011**, *36*, 2693–2700. [CrossRef]

55. Jayasinghe, P.; Hawboldt, K. A review of bio-oils from waste biomass: Focus on fish processing waste. *Renew. Sustain. Energy Rev.* **2012**, *16*, 798–821. [CrossRef]

56. Sakthivel, R.; Ramesh, K.; Purnachandran, R.; Shameer, P.M. A review on the properties, performance and emission aspects of the third generation biodiesels. *Renew. Sustain. Energy Rev.* **2018**, *82*, 2970–2992. [CrossRef]

57. Mansir, N.; Teo, S.H.; Mijan, N.-A.; Taufiq-Yap, Y.H. Efficient reaction for biodiesel manufacturing using bi-functional oxide catalyst. *Catal. Commun.* **2021**, *149*, 106201. [CrossRef]

58. Boycheva, S.; Zgureva, D.; Shoumkova, A. Recycling of lignite coal fly ash by its conversion into zeolites. *Coal Combust. Gasif. Prod.* **2015**, *7*, 1–8.

59. Faria, D.N.; Cipriano, D.F.; Schettino, M.A., Jr.; Neto, A.C.; Cunha, A.G.; Freitas, J.C. Na, Ca-based catalysts supported on activated carbon for synthesis of biodiesel from soybean oil. *Mater. Chem. Phys.* **2020**, *249*, 123173. [CrossRef]

60. Saifuddin, N.; Samiuddin, A.; Kumaran, P. A review on processing technology for biodiesel production. *Trends Appl. Sci. Res.* **2015**, *10*, 1. [CrossRef]

61. Leung, D.Y.; Wu, X.; Leung, M.K.H. A review on biodiesel production using catalyzed transesterification. *Appl. Energy* **2010**, *87*, 1083–1095. [CrossRef]

62. Anastopoulos, G.; Zannikou, Y.; Stournas, S.; Kalligeros, S. Transesterification of vegetable oils with ethanol and characterization of the key fuel properties of ethyl esters. *Energies* **2009**, *2*, 362–376. [CrossRef]

63. AMSEC. Rheometer Concise Operating Procedures. Available online: https://amsec.wwu.edu/files/2020-08/Rheometer_SOPs.pdf (accessed on 15 June 2022).

64. Lucas, J. How do I Determine the Free Fatty Acid (FFA) Percentage in Non-Edible Oils? Available online: https://www.researchgate.net/post/how_do_i_determine_the_Free_Fatty_Acid_FFA_Percentage_in_non-edible_oils (accessed on 15 June 2022).

65. Babajide, O.O. Optimisation of Biodiesel Production via Different Catalyic and Process Systems. Ph.D. Thesis, University of the Werstern Cape, Cape Town, South Africa, 2011.

66. Japir, A.A.-W.; Salimon, J.; Derawi, D.; Bahadi, M.; Al-Shuja'a, S.; Yusop, M.R. Physicochemical characteristics of high free fatty acid crude palm oil. *OCL* **2017**, *24*, D506. [CrossRef]

67. Ramírez-Verduzco, L.F.; Rodríguez-Rodríguez, J.E.; del Rayo Jaramillo-Jacob, A. Predicting cetane number, kinematic viscosity, density and higher heating value of biodiesel from its fatty acid methyl ester composition. *Fuel* **2012**, *91*, 102–111. [CrossRef]

68. Malonda Shabani, J.; Babajide, O.; Oyekola, O.; Petrik, L. Synthesis of Hydroxy Sodalite from Coal Fly Ash for Biodiesel Production from Waste-Derived Maggot Oil. *Catalysts* **2019**, *9*, 1052. [CrossRef]

69. World of Science. Product. Available online: https://worldofscience.co.za/product/sodium-hydroxide-ar-500g/ (accessed on 15 September 2022).

70. CCT. Water and sanitation services and costs in formal housing. Available online: https://www.capetown.gov.za/Family%20and%20home/residential-utility-services/residential-water-and-sanitation-services/water-and-sanitation-services-and-costs-for-formal-housing (accessed on 6 June 2022).

71. Hong, J.L.X.; Maneerung, T.; Koh, S.N.; Kawi, S.; Wang, C.-H. Conversion of coal fly ash into zeolite materials: Synthesis and characterizations, process design, and its cost-benefit analysis. *Industrial & Engineering Chemistry Research* **2017**, *56*, 11565–11574.